

Missing energy in black hole production and decay at the Large Hadron Collider

Douglas M. Gingrich

*Centre for Particle Physics, Department of Physics, University of Alberta,
Edmonton, AB T6G 2G7 Canada, and
TRIUMF, Vancouver, BC V6T 2A3 Canada
E-mail: gingrich@ualberta.ca*

ABSTRACT: Black holes could be produced at the Large Hadron Collider in TeV-scale gravity scenarios. We discuss missing energy mechanisms in black hole production and decay in large extra-dimensional models. In particular, we examine how graviton emission into the bulk could give the black hole enough recoil to leave the brane. Such a perturbation would cause an abrupt termination in Hawking emission and result in large missing-energy signatures.

KEYWORDS: Large Extra Dimensions, Black Holes.

JHEP11(2007)064

Contents

1. Introduction	1
2. Black hole production and decay	3
2.1 Gravitational radiation during black hole formation	4
2.2 Gravitational radiation after black hole formation	5
3. Hawking evaporation	6
3.1 Degrees of freedom	6
3.2 Emission spectra and probabilities	7
4. Binding of the black hole to the brane	10
5. Black hole recoil model and simulation	11
6. Results	14
6.1 Graviton	14
6.2 Recoil effect	15
6.3 Multiplicities	17
6.4 Missing energy	19
6.5 Mass and cross section	21
7. Discussion	23

1. Introduction

Models of large extra dimensions allow the fundamental scale of gravity to be as low as the electroweak scale [1–3]. If the gravity scale is as low as a TeV, black holes could be produced in collisions at the Large Hadron Collider (LHC). Once formed, the black hole will decay by emitting Hawking radiation [4]. In these models, our universe has a domain wall structure, the brane, that is embedded in a higher-dimensional bulk spacetime. In the class of models we will consider, the Standard Model particles are confined to the brane while the graviton is allowed to exist in all the dimensions. Graviton emission would be observed as missing energy and, if the recoil given to the black hole is significant, may result in the black hole leaving the brane during the decay process.

Numerous authors have estimated an enormous black hole production rate of about 10^7 per year at the LHC. This large rate is due to an anticipated parton-parton cross section that rises geometrically with increasing parton-parton centre of mass energy, and the assumption that all partons partake equally in black hole formation. Only the steeply

falling parton's momentum distribution in the proton keep the cross section reasonably finite.

There are several ways to reduce the black hole cross section yet still allow black holes to be produced at the LHC. The classical parton cross section will probably not hold at parton-parton collision energies near the fundamental Planck scale M_{P} . It is possible that the LHC will operate in the regime in which the effects of quantum gravity can not be ignored. In the quantum regime, the black hole may become stringy (string ball) and have a different cross section energy dependence [5, 6]. Even if we are well above the Planck scale and clear of the effects of quantum gravity, it has recently been pointed out that the contribution to the stress energy tensor in Einstein's equations due to charged, and perhaps coloured, partons will prevent all partons in the proton from contributing equally to black hole production [7, 8]. Some charged partons may not contribute at all under certain kinematic conditions and regions of higher-dimensional parameter space.

Perhaps the largest uncertainty in the classical black hole cross section picture is due to gravitational radiation during black hole formation. Apparent-horizon studies give lower bounds on the amount of energy that could be trapped behind the horizon during black hole formation [9, 10]. Although it is not known how much of the lower bound is due to the apparent-horizon technique, results in four dimensions indicate that significant radiation could be emitted [11]. Assuming the black hole cross section is a function of the black hole mass, initial radiation could significantly lower the production cross section. Even if the black hole is considered to have formed before the radiation is emitted, the gravitational radiation will result in missing energy, and the black hole will effectively have a lower mass before it begins to be detectable by its Hawking radiation on the brane.

It has long been argued that if black holes are produced at the LHC, they will give rise to spectacular decay signatures [12–14]. The Hawking evaporation of these very hot black holes is expected to generate high-multiplicity, almost spherical events with several very high-energy jets, high- p_{T} leptons, and possibly even exotic particles [15]. Black holes could also be identified by their large missing-energy signatures from high-energy neutrinos emitted in the evaporation process. However, large missing-energy events need to be removed from the data sample, or well understood, to enable an accurate reconstruction of the black hole mass [16, 17]. It is the measurement of the black hole mass and event rate that will allow us to infer the Planck scale, and possibly, the number of extra dimensions.

There are additional missing-energy signatures that could make the reconstruction of black holes extremely difficult. It is not known how the evaporation process will end. The possibility of a final black hole remnant with mass of the order of the Planck scale has been studied [18]. Either this remnant is charged and ionizing like a particle, in which case it will need to be detected, or more likely [19], it will be neutral and possibly not detectable.

A final possibility giving missing energy, that we will examine, is that the black hole will be perturbed during the decay process and could leave the brane. If the black hole escapes, it will result in large missing energy. It is unlikely that the black hole would leave the brane at a particular mass value, but it will probably be a stochastic process depending on the initial black hole mass and the history of the evaporation process. Such a phenomena may assist in black hole identification, but it might make accurate kinematic

reconstruction of the black hole mass difficult. Hawking radiation is thermal and leads to unique democratic signatures, but it is not clear if these signatures could be identified for those events in which the black hole leaves the brane.

With all these missing-energy signatures, we argue that it may be difficult to conclusively detect black holes if they are produced at the LHC. Since a black hole is not a mass resonance, we will not know *a priori* what initial energy went into the black hole formation; energy will be lost during the production process. Once formed, black hole states may be difficult to accurately reconstruct event by event from the final-state particles because of widely varying missing energy in the decay process.

In this paper, we discuss missing energy due to mechanisms that are not usually mentioned in the literature on TeV-scale black hole production and decay. We concentrate our study on missing energy from Schwarzschild black holes that leave the Standard Model brane during the Hawking evaporation process. An outline of this paper is as follows. In section 2 we discuss qualitatively black hole production and decay with particular emphasis on the graviton radiation processes. In section 3 we review the Hawking evaporation process in higher dimensions with particular attention to the graviton mode. We briefly review a mechanism for black hole escape from the brane and a model of the binding potential in section 4. In section 5 we describe our model and simulation. Graviton emission probabilities, particle multiplicities, and the probability for the black hole to leave the brane, along with missing energy distributions and their effect on the black hole mass and cross section are examined in Sec 6. In section 7 we conclude with a discussion.

2. Black hole production and decay

Black hole production and decay can be thought of as evolving according to a series of distinct phases. In the production phase, the gravitational fields of the relativistic particles producing the black hole are approximately localized to narrow longitudinal shock waves and spacetime is flat before the collision. At the instance of collision, the two shock waves pass through one another, and interact nonlinearly by shearing and focusing. After the collision, the two shocks continue to interact nonlinearly with each other and spacetime within the future lightcone of the collision becomes highly curved. A complex-shaped event horizon forms which quickly collapses down to a more regular-shaped apparent horizon by the emission of gravitational waves into the bulk space. Not all the energy in the two-particle collision is trapped behind the horizon and the collision process can be considered to be inelastic. The effect of inelasticity is to reduce the black hole mass and thus cross section, but otherwise does not give observable signatures. The black hole produced may have any gauge or angular momentum quantum numbers arising from the two initial partons.

According to the no-hair theorem [20], the resulting asymmetry and moments due to the violent production process are radiated away by gravitons into the bulk until a Kerr-Newman stationary solution is formed, which is characterized by only its mass, angular momentum, and local charges (electric charge and probably colour charge). For excited black holes produced in four dimensions by neutral relativistic particles, 16% of the total energy is lost in this balding phase [11].

Due to conservation of angular momentum, the angular momentum of the formed black hole can only vanish completely for central collisions with zero impact parameter. In the general case of an impact parameter, there will be an angular momentum. Black holes are expected to be produced in high angular-momentum states from particle collisions above the Planck scale. It is anticipated that they will spin down by Hawking evaporation very rapidly to Reissner-Nordström static solutions by the emission of high-spin state particles. In four dimensions, the half-life of the spin down phase is 7% of the black hole lifetime, and about 25% of the mass is lost during this spin-down phase [21]. The various emissivities are enhanced by a factor of about 35 to almost 100 as the number of dimensions increase; this factor increases by 3 to 6 as the angular momentum of the black hole increases [22]. In higher dimensions, black holes also tend to lose their angular momentum at the early stage of evolution. However, black holes can still have a sizable rotation parameter after radiating half their mass. Typically more than 70% to 80% of the black hole's mass is lost during the spin-down phase [23].

The Schwarzschild evaporation phase (Hawking evaporation of a non-rotating black hole) is the most well studied. A black hole of a particular mass is characterized by a Hawking temperature and, as the decay progresses, the black hole mass falls and the temperature rises. Thermal radiation is thought to be emitted by black holes due to quantum effects. Grey-body factors modify the spectrum of emitted particles from that of a perfect thermal black body [24] and quantify the probability of transmission of the particles through curved spacetime outside the horizon. At high energies, the shape of the spectrum is like that of a black body while at low energies the behaviour of the grey-body factors is spin-dependent and also depends on the number of dimensions.

Baryon number (B) and lepton number (L) do not have to be conserved in black hole decay. However, it is widely believed that $B - L$ is conserved, which would help bind the black hole to the brane.

Since Hawking radiation allows black holes to lose mass, they could evaporate, shrink, and ultimately vanish. A black hole can not decay down to nothing without the loss of information. Another possibility is that a black hole could leave a sub-Planckian remnant. The final fate of a black hole is unknown since quantum gravity will become important as the black hole mass approaches the Planck scale.

2.1 Gravitational radiation during black hole formation

It is not known at what instance a black hole would form in particle collisions in low-scale gravity scenarios. During the formation process, significant amounts of gravitational radiation would probably be emitted. Likewise, significant gravitational radiation could be emitted near the threshold for black hole formation even if the black hole does not form.

Pretorius and Khurana [25] have performed numerical studies in four dimensions of black hole mergers and unstable circular orbits for a class of equal-mass, non-rotating, non-circular binary black hole systems in general relativity. They find evidence of an approximate correspondence between near-threshold evolution of geodesics and generic binary merger. They applied this correspondence to the threshold for black hole production in particle collisions of high energy. The merger of two black holes is thought to be equivalent

to black hole formation in particle collisions of sufficiently high energy where the classical general relativistic description holds. Ideally we would like to know the threshold impact parameter below which a black hole forms and the energy radiated as a function of impact parameter. Pretorius and Khurana find that at threshold it is possible that essentially all the kinetic energy is radiated as gravitational waves and that there is still significant energy loss to gravitational waves for impact parameters up to almost twice the critical value for black hole formation. Although these studies are in four dimensions, no counter arguments have been made to indicate that they are not applicable in higher dimensions.

Since black hole production at the LHC mostly occurs from quark-quark interactions, most of the produced black holes will have fractional electric charge and colour. These quantum numbers will make it difficult for the black hole to leave the brane before this hair can be shed during the balding phase.

2.2 Gravitational radiation after black hole formation

During the balding phase, the black hole is considered to exist. The black hole settles down into a Kerr-Newman solution by eliminating its moments in gravitational radiation. Although Kerr-Newman solutions are unique in four dimensions this is not the case in higher dimensions [26, 27]. Indeed, black hole Saturn solutions have been found in five dimensions and are anticipated to exist in other higher dimensions.

It will be difficult to obtain experimental information about black hole formation and the balding phase; all emitted radiation is undetectable gravitational waves formed from partons of unknown initial energies. Gravitational radiation will result in lowering the black hole mass before the spin-down phase begins. Thus measurement of the cross section may have to be corrected for gravitational radiation by theory and modeling in order to obtain the true mass dependence. This situation is not dissimilar to electromagnetic or QCD initial-state radiation in which the radiation can not be detected. To make the correction more difficult, the black hole is not a particle with a definite mass and the amount of radiation has not yet been formulated.

Black holes are expected to be highly rotating when produced in particle collisions. A black hole can thus exhibit superradiance in its decay. This enhances the emission of higher spin-state particles possibly making the emission of gravitons a dominant effect. In four dimensions, Page [21] showed that the probability of emission of a graviton by an extremely rotating black hole is 100 times higher than the probability of emission of a photon or a neutrino. In four dimensions, graviton emission, which is suppressed for small rotations, rapidly increases with angular momentum, but the angular momentum is restricted to $J < M^2$. In higher dimensions, there is no upper bound on J and so graviton emission could dominate the evaporation process for rotating black holes.

Since gravitons are not bound to the brane, most would radiate into the bulk. Although black holes produced at the LHC would initially have no components of angular momentum in the higher dimensions, the bulk components would soon become nonzero due to graviton emission. A rotating black hole could lose its bulk components of rotation by interacting with the brane or emitting further Hawking quanta into the bulk. Emission of gravitons

into the bulk during the spin-down phase could thus strongly perturb the system, possibly causing the black hole to leave the brane.

3. Hawking evaporation

Hawking radiation provides distinct experimental signatures that may allow discrimination between gravitational events and other perturbative non-gravitational physics. For an uncharged, non-rotating black hole, the decay spectrum per degree of freedom s is described by

$$\frac{dN^{(s)}(\omega)}{dt d\omega} = \frac{1}{2\pi} \frac{\Gamma^{(s)}(\omega)}{\exp(\omega/T_H) \mp 1}, \quad (3.1)$$

where ω is the energy of the emitted quanta, T_H is the temperature of the black hole, and $\Gamma^{(s)}(\omega)$ is the grey-body factor for mode s . The last term in the denominator is a spin-statistics factor which is -1 for bosons or $+1$ for fermions. Equation (3.1) refers to individual degrees of freedom not elementary particles. However, it can be used to determine the decay spectrum for a particular particle by summing over the number of degrees of freedom.

It has been thought that the majority of the energy in Hawking radiation is emitted into Standard Model particles, but a small amount is also emitted into gravitons [28]. A common argument in support of this claim is that fewer particles are emitted in the bulk than on the brane; only the graviton is emitted in the bulk, whereas all the Standard Model fields are emitted on the brane. However, the emission rate per degree of freedom of the graviton in the D -dimensional bulk could be higher than that of the four-dimensional brane modes. It is now thought that the probability of emitting spin-two quanta in high dimensions is substantial [29].

In four dimensions, the graviton power loss is negligible compared to the loss in Standard Model channels. The Standard Model emissivities should not change much in higher dimensions while the graviton emissivity is expected to be higher in higher dimensions due to the increase in number of helicity states. In four dimensions, gravitational waves have two possible helicities. In D dimensions, the number of helicities is

$$\mathcal{N} = \frac{D(D-3)}{2}. \quad (3.2)$$

Thus in 11 dimensions the number of graviton helicity states reaches 44. In addition, the total power radiated in gravitons increases more rapidly than the power radiated in lower-spin fields as the number of dimensions increases. This is due to the increase in the multiplicity of the tensor perturbations [29–31].

3.1 Degrees of freedom

We assume the particle content at trans-Planckian energies will be the minimal $U(1) \times SU(2) \times SU(3)$ Standard Model with three families and one Higgs field. The number of degrees of freedom (dof) for each particle is given by

$$\text{dof} = n_Q \times n_S \times n_F \times n_C, \quad (3.3)$$

Particle Type	Charge States	Spin States	Flavour States	Colour States	dof
quarks	2	2	6	3	72
charged leptons	2	2	3		12
neutrinos	2	1	3		6
gluons	1	2		8	16
photon	1	2			2
Z boson	1	3			3
W bosons	2	3			6
Higgs	1				1
graviton	1				1

Table 1: Number of degrees of freedom (dof) of the Standard Model particles.

where n_Q is the number of charge states, n_S the number of spin polarizations, n_F the number of flavours, and n_C the number of colours. Not all these degrees of freedom apply to each type of particle. For massive gauge bosons one of their degrees of freedom comes from the Higgs mechanism. This means for each massive gauge boson there is one spin-0 degree of freedom and two spin-1 degrees of freedom. The number of degrees of freedom for each Standard Model particle is shown in table 1. The number of degrees of freedom (helicities) for the graviton will be accounted for in the emissivity since it depend on the number of dimensions.

The picture of a massless graviton propagating in D dimensions and the picture of massive Kaluza-Klein (KK) gravitons propagating in four dimensions are equivalent. The $D(D - 3)/2$ helicity states of the massless graviton in D dimensions can be decomposed into KK helicity states: 1 scalar state, $(D - 3)$ vector states, and $(D - 4)(D - 1)/2$ tensor states.

The KK picture allows one to write down an effective theory of interactions of KK gravitons with Standard Model particles. This effective theory will breakdown above the Planck scale where black holes are active. The gravitons propagate in the extra dimensions and can decay into ordinary particles only by interacting with the brane, and therefore with a rate suppressed by $1/M_p^2$. The KK excitations of the graviton have the same very weak coupling to the Standard Model fields as their massless zero mode. This is because the graviton decaying weakly to ordinary matter is not compensated by the large phase space of KK states. We will thus assume the KK gravitons behave like massive, non-interacting, stable particles, and that this assumption also holds in the trans-Planckian region. KK states can be produced in Standard Model particle collisions with a reasonable strength. Like all previous work on Hawking evaporation, we ignore the interactions of all particles, including the KK gravitons. We will also ignore possible light Nambu-Goldstone fields related to the brane dynamics.

3.2 Emission spectra and probabilities

In the following, we will need the relative emission rates and the shapes of the emission

spectra. The flux spectrum (number of particles emitted per unit time) is given by¹

$$\frac{dN^{(s)}(\omega)}{dt} = \sum_l \sigma_{n,l}^{(s)}(\omega) \frac{1}{\exp(\omega/T_H) \mp 1} \frac{d^{n+3}k}{(2\pi)^{n+3}}, \quad (3.4)$$

where

$$\sigma_{n,l}^{(s)}(\omega) = \frac{2^n \pi^{(n+1)/2} \Gamma[(n+1)/2] (2l+n+1)(l+n)!}{n! \omega^{n+2} l!} \left| \mathcal{A}_l^{(s)}(\omega) \right|^2 \quad (3.5)$$

is the grey-body factor for an $(n+4)$ -dimensional Schwarzschild black hole. The quantity $\sigma_{n,l}^{(s)}(\omega)$ is alternatively called the partial absorption cross section. It is the absorption (or transmission) probability for a scalar particle propagating in the brane background. For a black body, $\sigma_{n,l}^{(s)}(\omega)$ is just a constant representing the area of the emitting body. The absorption coefficient $\mathcal{A}_l^{(s)}(\omega)$ is not the grey-body factor. Equation (3.4) is for a non-rotating, non-charged black hole. For a rotating or charged black hole, the argument of the exponential is replaced by a more general expression.

For massless particles, we can integrate over the solid angle to obtain the flux spectrum

$$\frac{dN^{(s)}(\omega)}{dt} = \sum_l \mathcal{N}_l \left| \mathcal{A}_l^{(s)}(\omega) \right|^2 \frac{1}{\exp(\omega/T_H) \mp 1} \frac{d\omega}{2\pi}, \quad (3.6)$$

where

$$\mathcal{N}_l = \frac{(2l+n+1)(l+n)!}{l!(n+1)!} \quad (3.7)$$

is the multiplicity of scalar modes for partial wave l . The sum in eq. (3.6) can be removed by writing

$$\frac{dN^{(s)}(\omega)}{dt} = \frac{\Gamma^{(s)}(\omega)}{\exp(\omega/T_H) \mp 1} \frac{d\omega}{2\pi}, \quad (3.8)$$

where

$$\Gamma^{(s)}(\omega) = \sum_l \mathcal{N}_l \left| \mathcal{A}_l^{(s)}(\omega) \right|^2. \quad (3.9)$$

This result is identical to the previous expression eq. (3.1). The relative probability for each particle to be produced is obtained by integrating the flux spectra. For black bodies (without grey-body factors), the relative probability for bosons to be produced is 1 and for fermions is 3/4.

The gravitational coupling is flavour blind and to first order a black hole emits all 118 Standard Model particle and antiparticle degrees of freedom with approximately equal probability. To obtain more accurate relative rates requires knowledge of the grey-body factors, including their full energy dependence. Many calculations of the grey-body factors have been performed. In four dimensions, the relative emissivities per degree of freedom for a non-rotating black hole are 1, 0.37, 0.11, and 0.01 for spin-0, 1/2, 1, and 2 modes. Kanti and March-Russell [32, 33] calculated the grey-body factors in higher dimensions analytically using a low-energy approximation. Harris and Kanti [34, 35] performed an

¹Throughout this paper we use D to represent the total number of spacetime dimensions, but in this section we use the common convention of n to represent the number of extra space dimensions: $D = (n+4)$.

D	4	5	6	7	8	9	10	11	BB
Higgs	1.00	1.00	1.00	1.00	1.00	1.00	1.00	1.00	1
fermions	0.37	0.70	0.77	0.78	0.76	0.74	0.73	0.71	0.75
gauge bosons	0.11	0.45	0.69	0.83	0.91	0.96	0.99	1.01	1
graviton	0.02	0.20	0.60	0.91	1.90	2.50	5.10	7.60	1

Table 2: Fractional emission rates per degree of freedom normalized to the scalar field [34, 42]. The graviton results include all the helicity states and count as one degree of freedom.

exact calculation of the grey-body factors numerically. Ida, Oda, and Park [23, 36, 37] have performed the calculation for rotating black holes. The rotating case has also been performed by sets of different authors [22, 38, 39].

Gravitons can be handled by considering weak perturbations from external fields. The perturbations are divided into scalar, vector, and tensor. Tensor perturbations exist only in greater than four dimensions. The total absorption cross section is obtained by summing the absorption coefficients $\mathcal{A}_l^{(s)}(\omega)$ for each mode l weighted by the multiplicity factors $\mathcal{N}_{n,l}^{(s)}$. For $n = 0$, $\mathcal{N}_{0,l}^{(S)} = \mathcal{N}_{0,l}^{(V)} = (2l + 1)$ and $\mathcal{N}_{0,l}^{(T)} = 0$. The total flux for gravitational waves is

$$\frac{dN}{dt} = \sum_{l=2}^{\infty} \int \frac{d\omega}{2\pi} \frac{1}{\exp(\omega/T_H) - 1} \left[\mathcal{N}_{n,l}^{(S)} \left| \mathcal{A}_l^{(S)}(\omega) \right|^2 + \mathcal{N}_{n,l}^{(V)} \left| \mathcal{A}_l^{(V)}(\omega) \right|^2 + \mathcal{N}_{n,l}^{(T)} \left| \mathcal{A}_l^{(T)}(\omega) \right|^2 \right], \quad (3.10)$$

where the counting of helicities is included in the multiplicity factors.

Again, knowledge of the grey-body factors is essential. Creek, Efthimiou, Kanti, Tamvakis [31] calculated the grey-body factors for gravitons in the bulk using an analytical approximation. Park [40] performed the calculation for gravitons on the brane. Cardoso, Cavagilá, Gualtieri [29, 41, 42] solved for the exact grey-body factors for gravitons in the bulk numerically.

Table 2 shows the fractional emission rates per degree of freedom normalized to the scalar field. The results for Standard Model particles are taken from ref. [34] while the results for gravitons are from ref. [42]. The emission rates for gravitons in higher dimensions are large, but the graviton results includes all the helicity states and count as one degree of freedom. We see that the emissivities for high dimensions are approximately those of a black-body (BB) spectrum, except in the case of the graviton.

The probabilities of emission for different particle types are given by

$$P_i = \frac{\epsilon_i \times \text{dof}_i}{\sum_j \epsilon_j \times \text{dof}_j}, \quad (3.11)$$

where ϵ_i and dof_i are the emissivity and number of degrees of freedom of particle i . Table 3 shows the probabilities for different particles types. We now see that graviton emission is significant but not dominant. Significant jets (quarks and gluons), very few photons, and insignificant Higgs bosons should be observed. Using table 3, we can estimate the types of signatures in a detector: 74% hadronic energy, 9% missing energy, 8% electroweak bosons, 6% charged leptons, 2% photons, and 1% Higgs bosons. The Standard Model particle

D	4	5	6	7	8	9	10	11	BB
quarks	0.71	0.66	0.62	0.59	0.57	0.55	0.53	0.51	0.56
charged leptons	0.12	0.11	0.10	0.10	0.10	0.09	0.09	0.09	0.09
neutrinos	0.06	0.06	0.05	0.05	0.05	0.05	0.04	0.04	0.05
gluons	0.05	0.09	0.12	0.14	0.15	0.16	0.16	0.16	0.17
photon	0.01	0.01	0.02	0.02	0.02	0.02	0.02	0.02	0.02
EW bosons	0.03	0.05	0.07	0.08	0.09	0.09	0.09	0.09	0.09
Higgs	0.03	0.01	0.01	0.01	0.01	0.01	0.01	0.01	0.01
graviton	0.00	0.00	0.01	0.01	0.02	0.03	0.05	0.08	0.01

Table 3: Probability of emission for different particles.

results are consistent with earlier results [43]. We conclude that jets will dominate black hole events while missing energy will be significant.

4. Binding of the black hole to the brane

Normally a black hole will not move into the bulk because it is likely to have charge, colour, or lepton/baryon number hair that will keep it on the brane. However, the emission of higher-dimensional gravitons will cause the black hole to recoil into the extra dimensions if there is no symmetry that suppresses the recoil.

Most studies of low-scale gravity models in large extra dimensions assume the so called probe-brane approximation. In this approximation, the only effect of the brane field is to bind the black hole to the brane, and that otherwise the black hole may be treated as an isolated object in the extra dimensions. The brane must intersect the black hole orthogonally [28]. To talk about a black hole escaping from the brane into the higher-dimensional bulk requires us to go beyond the probe-brane approximation.

There are two main approaches used to study the escape of a black hole from the brane. One is to model the domain wall as a field-theoretical topological defect. The phenomena of escape is thus studied by treating the brane as a domain wall in a scalar effective field theory. Another approach is to treating the brane in the Dirac-Nambu-Goto approximation, and analyze the problem by studying the interaction between a Dirac-Nambu-Goto brane and a black hole assuming adiabatic (quasi-static) evolution.

The recoil of a black hole was studied by Frolov and Stojković [44–46] within a toy model consisting of two scalar fields, one describing the black hole and the other a possible quanta emitted by the black hole in the process of evaporation. The interaction with the brane was approximated as weak, and it was shown that as soon as a quanta was emitted in the extra dimensions, the black hole left the brane. In their study, it is not clear how the separation process occurs. Flachi *et al.* [47] examined the problem further by studying the interaction of a small black hole and a domain wall composed of a scalar field, and simulated the evolution of the system when the black hole acquires an initial recoil velocity.

Flachi and Tanaka [48] studied the dynamics of Dirac-Nambu-Goto branes in black hole spacetimes and suggested a mechanism for the escape of the black hole based on

reconnection of the brane. Once the black hole acquires an initial recoil velocity perpendicularly to the brane, an instability develops and the brane tends to envelop the black hole. These results were obtained in the approximation that the tension of the brane has no self-gravity effect. While ignoring the tension is reasonable when the recoil velocity is large, it might not be so in the opposite case of small recoil velocity. The configuration with a black hole on a brane is stable under a perturbation causing a small recoil velocity.

When the tension of the brane is large, the deformation of the geometry caused by the gravity of the brane needs to be taken into account. It is not clear if the brane tension will prevent the black hole from escaping for small recoil velocities. Flachi *et al.* restricted their considerations to effects which are lowest order in the brane tension next to the probe-brane approximation. A critical escape velocity was found and thus it is possible the black hole could leave the brane before evaporation is complete if the initial mass of the black hole is large. Even if the black hole leaves the brane, it feels a restoring force due to the brane tensions and is not likely to move very far.

The height of the energy barrier for escape is approximately [49]

$$\mathcal{O}\left(\sigma(G_D M)^{3/(D-3)}\right), \tag{4.1}$$

where M is the black hole mass, G_D is the D -dimensional Newton constant, and σ is the brane tension. Using the Dimopoulos and Landsberg definition of $G_D = 1/M_P^{D-2}$, where M_P is the fundamental Planck scale ($\sim \text{TeV}$), we can write the barrier energy as

$$V = \sigma \left(\frac{1}{M_P}\right)^3 \left(\frac{M}{M_P}\right)^{\frac{3}{D-3}}. \tag{4.2}$$

Typically we expect $\sigma \sim M_P/l^3$, where the length is $l \sim 1/M_P$. This gives $\sigma \sim M_P^4$. Defining the dimensionless tension

$$\hat{\sigma} = \left(\frac{1}{M_P^4}\right)\sigma, \tag{4.3}$$

we write

$$V = \hat{\sigma} M_P \left(\frac{M}{M_P}\right)^{\frac{3}{D-3}}, \tag{4.4}$$

where $\hat{\sigma}$ is of order 1. To leave the brane, a black hole must have a momentum p_\perp transverse to the brane given by

$$p_\perp > \sqrt{V(V + 2M)}. \tag{4.5}$$

We ignore the rare possibility of a black hole reentering the brane after escaping to the bulk. Such scenarios have been examined by Dvali *et al.* [50].

5. Black hole recoil model and simulation

To study the effects of missing energy in black hole decay, we have constructed a simple model. All Standard Model particles evaporating from the black hole do so in four dimensions. The graviton evaporates off the black hole in D dimensions. We assume the

evaporated particles are non-interacting so that the graviton is free to move in the extra dimensions without impediment just like the Standard model particles move in four dimensions. We also assume the graviton is massless and does not decay or otherwise interact in the bulk. This approximation is justified when the tension of the brane is small so that the interaction between the Nambu-Goldstone boundary fields and the KK modes is exponentially suppressed. Soft branes also reduce graviton interactions with Standard Model particles [51].

In our model, the black hole is treated differently because of its mass and is bound to the brane by a brane tension according to the model of ref. [47–49]. We perform the decay kinematics in D dimensions and keep track of the black hole recoil momentum transverse to the brane. If this momentum exceeds the binding potential of the black hole to the brane (eq. (4.5)), the black hole is considered to have escaped from the brane; the decay process is stopped and the missing energy is recorded.

Details of the horizon formation, balding, and spin-down phases have been ignored. The important effects of angular momentum in the production and decay of the black hole in extra dimensions are not taken into account. Our black holes can be considered as D -dimensional Schwarzschild solutions.

We implemented the Hawking evaporation phase in two steps: determination of the particle types and assigning energy to the decay products. Particle types are randomly selected with a probability determined by their number of degrees of freedom and the ratio of emissivities. To pick between a particle or antiparticle, the emitted charge and baryon number are chosen such that the magnitude of the black hole charge and baryon number does not increase after a particle is emitted, else particles and antiparticles are chosen with equal probability. All Standard Model particles are considered included a Higgs².

The energy assigned to the decay particles in the evaporation phase has been implemented as follows. The particle type selected as described by the model above is given a random energy according to its decay spectrum. A different decay spectrum is used for scalars, fermions, and vector bosons, i.e. the spin statistics factor is taken into account. Grey-body factors for Standard Model particles are used without approximations [34]. Spectra for massless particles are used, even for the gauge bosons and heavy quarks. This is a good approximation provided the top-quark mass $m_t \ll T_H$. The Hawking temperature is updated after each particle is emitted. This assumes the decay is quasi-stationary in the sense that the black hole has time to come to equilibrium at each new temperature before the next particle is emitted. The energy of the particle given by the spectrum must be constraint to conserve energy and momentum at each step.

The evaporation phase ends when the black hole mass drops below the Planck scale. When this occurs, a final isotropic two-body phase-space decay is performed. The black hole decays totally to Standard Model particles and/or gravitons. Overall electric charge, baryon number, and colour are conserved in the black hole production and decay.

If the black hole escapes from the brane during evaporation, up to two partons with the black hole charge and baryon number are added to the event record with zero momentum.

²Include the scalar Higgs is not significant since it has only one degree of freedom in all dimensions.

Name	Description	Value
MINMSS	Minimum mass of black holes	5 GeV
MAXMSS	Maximum mass of black holes	14 GeV
MPLNCK	Planck scale	1 GeV
MSSDEF	Planck scale definition	2
TOTDIM	Total number of dimensions	6, 8, or 11
NBODY	Number of particles in remnant decay	2
GTSCA	Black hole mass used as PDF momentum scale	true
TIMVAR	Allow T_H to change with time	true
MSSDEC	Use all SM particles as decay products	true
GRYBDY	Include grey-body effects	true
KINCUT	Use a kinematic cut-off on the decay	false

Table 4: Parameters use in the CHARYBDIS generator.

In this way, we can complete the colour connection, yet still account for missing energy.

To implement our model, we started from the Monte Carlo event generator CHARYBDIS version 1.003 [52, 53] and adapted it for our study. It was interfaced to PYTHIA which provides the parton evolution and hadronization, as well as Standard Model particle decays. The interface to PYTHIA or HERWIG is not important since the studies presented here are at the particle level. Gravitons were added as a particle type and the kinematics for the evaporation of the graviton from the black hole were calculated in D dimensions. The condition for escape from the brane was examined after each graviton was emitted. Table 4 lists the CHARYBDIS parameter settings.

The graviton is represented by a zero charged, non-interacting, massless particle in D dimensions. The $(D - 4)$ extra dimensions are represented internally in CHARYBDIS and are not known to PYTHIA or appear in the event record. The black hole is also treated as a D -dimensional particle internally in CHARYBDIS. The black hole is not added to the event record since it decays entirely in CHARYBDIS. See Koch, Bleicher, Hossenfelder [18] for an alternative formulation.

The charge and baryon number of the black hole are recalculated after each particle is emitted. The final two-body decay must generate two particle that have the charge and baryon number of the black hole. Sometimes the black hole will have too high an absolute charge or baryon number so that a two-body final state is not possible. We thus encourage the absolute charge and baryon number of the black hole not to become too large by choosing between particle or antiparticle states to minimize the absolute charge and baryon number of the black hole after each decay. For example, a quark or anti-quark will be chosen to reduced the absolute value of the black hole baryon number after the decay. A similar difficulty can occur when the black hole leaves the brane with a large charge or baryon number. We need to include a number of zero-energy quarks or anti-quarks in the event to allow the colour connection to be made.

If the black hole does not leave the brane, a final two-body decay is performed. Three possibilities exist for the final decay: 1) both particles are Standard Model particles,

CHARYBDIS performs a normal decay in four dimensions, 2) one is a Standard Model particle and one is a graviton, CHARYBDIS performs the decay in four dimensions, and 3) both particles are gravitons, a two-body decay is performed in D dimensions. The special case 2) of the graviton being restricted to four dimensions is not important since there is no longer a black hole to recoil against it. In any case, gravitons will appear as missing energy on the brane.

6. Results

We present results for black holes with $5 < M < 14 \text{ TeV}$ and $M_{\text{P}} = 1 \text{ TeV}$. Since the cross section falls steeply with increasing black hole mass, most of the black holes will have a mass close to 5 TeV while very few will have a mass above 9 TeV. Most results will be presented in 11 dimensions but sometimes six and eight dimensions will be used for comparison. Normally we examine the results under two extreme choices of brane tension: vanishing tension $\hat{\sigma} = 0$ and strong tension $\hat{\sigma} = 10^3$.

6.1 Graviton

We studied the effects of adding the graviton to CHARYBDIS by examining the distribution of particle types from black hole decay. CHARYBDIS relies on conserving overall charge and baryon number in the final decay. Differences from the probabilities in table 3 can be due to requiring charge and baryon number conservation, as well as energy-momentum conservation. To study these asymmetries, we first generated $p\bar{p}$ collisions with black-body spectra for the emitted particles. We eliminated the need to conserve overall charge, baryon number, and energy-momentum in the Hawking evaporation. The fractional occurrences of the different particle types were as expected (table 3) to an accuracy better than 0.8%.

Having simulated the relative frequency of occurrence for different particles in Hawking evaporation according to expectations, we simulated pp collisions and included grey-body factors, as well as the two-body final decay. The resulting frequency of occurrence of each particle type is shown in figure 1. The simulated results are shown as the black histogram and the expectations, according to black-body spectra in four dimensions, as the red histogram. We see that quarks are enhanced over anti-quarks and gluons in order to conserve the normally positive baryon number of the initial state. Similarly, positive charged quarks and anti-quarks are enhanced over negative charged particles in order to conserve the normally positive net charge of the black hole. Differences between the simulation and black-body democracy can be as high as 80%. The graviton frequency of occurrence is more than 660% times higher than that predicted by the black-body spectrum in four dimensions. Besides the asymmetries due to grey-body factors, asymmetries occur during the two-body final decay. If there is a need to conserve other quantum numbers, like lepton number, further asymmetries will result.

The emissivity of gravitons in D dimensions has been calculated [41, 42]. What is not known, or readily available, is the shape of the decay spectrum for gravitons. The Standard Model flux spectra [34] are shown in figure 2. Each spectrum has been normalized to unit area. We see that the relative shapes of the spectra are similar except for the grey-body

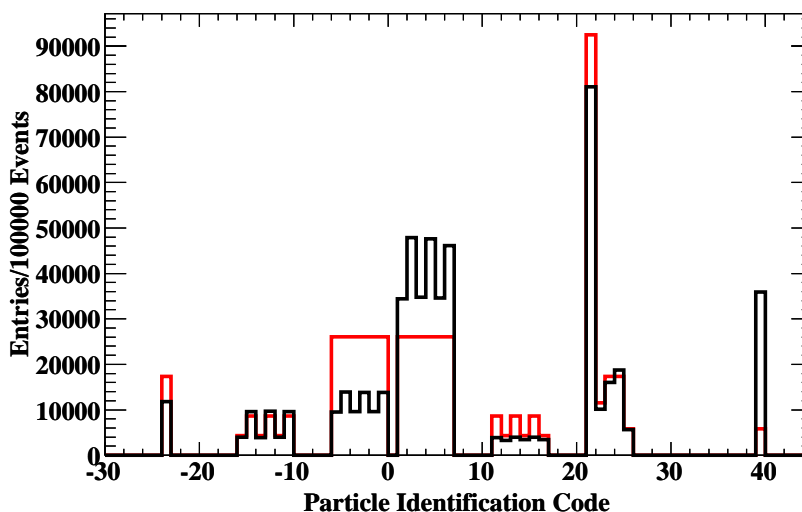


Figure 1: Frequency of occurrence of each particle type (particle identification code) for black holes with $5 < M < 14$ TeV, $M_P = 1$ TeV, and $D = 11$. The simulated results are shown as the black histogram while the black-body expectations are shown as the red histogram. The positive particle identification codes are 1 d-quark, 2 u-quark, 3 s-quark, 4 c-quark, 5 b-quark, 6 t-quark, 11 e^- , 12 ν_e , 13 μ^- , 14 ν_μ , 15 τ^- , 16 ν_τ , 21 gluon, 22 photon, 23 Z, 24 W^+ , 25 Higgs, 39 graviton. The negative particle identification codes are the antiparticles.

spin-1 case. They are most similar in seven extra ($D = 11$) dimensions and the grey-body spin-1/2 case is a typical spectrum. The shape of the grey-body spectrum for spin-1/2 particles was used for the graviton. The sensitivity to this arbitrary choice is examined in section 6.4.

6.2 Recoil effect

We can ask at what point during Hawking evaporation we would expect the black hole to be sufficiently perturbed to leave the brane? Assuming the kinetic energy must be greater than the barrier potential, the critical perpendicular velocity for a black hole to leave the brane is

$$v_c = \sqrt{\hat{\sigma}} \left(\frac{M_P}{M} \right)^{\frac{D-6}{2(D-3)}}. \quad (6.1)$$

The average black hole recoil velocity after evaporating off a particle is of the order [49]

$$v_r = \left(\frac{M_P}{M} \right)^{\frac{D-2}{2(D-3)}}. \quad (6.2)$$

Thus the black hole would leave the brane when $v_r \gtrsim v_c$ which should occur at the critical mass

$$M \lesssim M_c = \frac{M_P}{\hat{\sigma}^{(D-3)/4}}. \quad (6.3)$$

If the initial mass of the black hole is greater than M_c , it may decay down to M_c . If the initial mass is below M_c , the black hole will probably leave the brane when the first

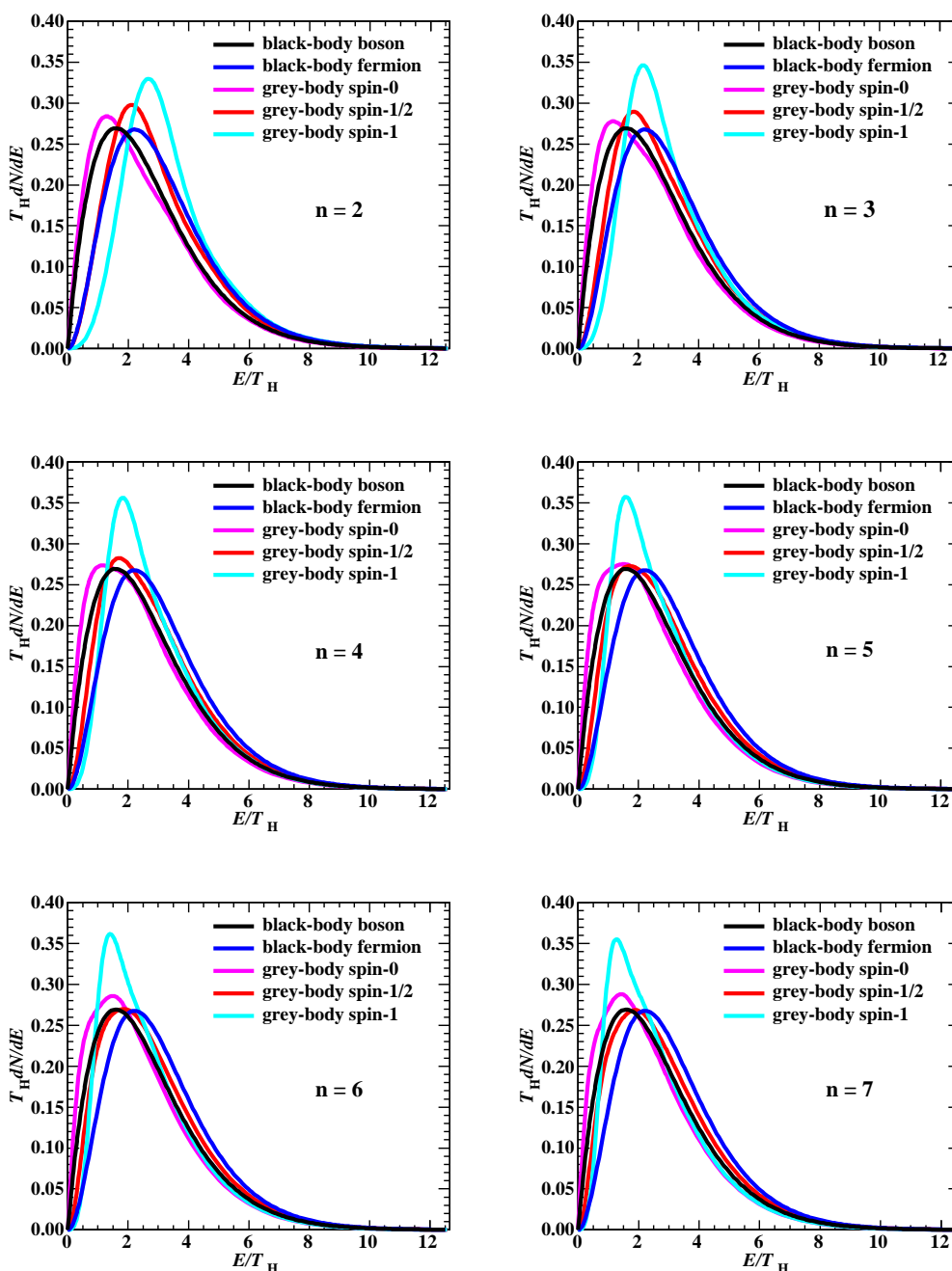


Figure 2: Energy spectra for grey bodies and black bodies [34]. Each spectrum has been normalized to unit area.

graviton is emitted. If the black hole minimum mass is above M_C , the black hole will not leave the brane. In our model, the minimal black hole mass is M_P , so the black hole will only leave the brane if $\hat{\sigma} \lesssim 1$.

Figure 3 shows the probability per event for a black hole with $5 < M < 14$ TeV and

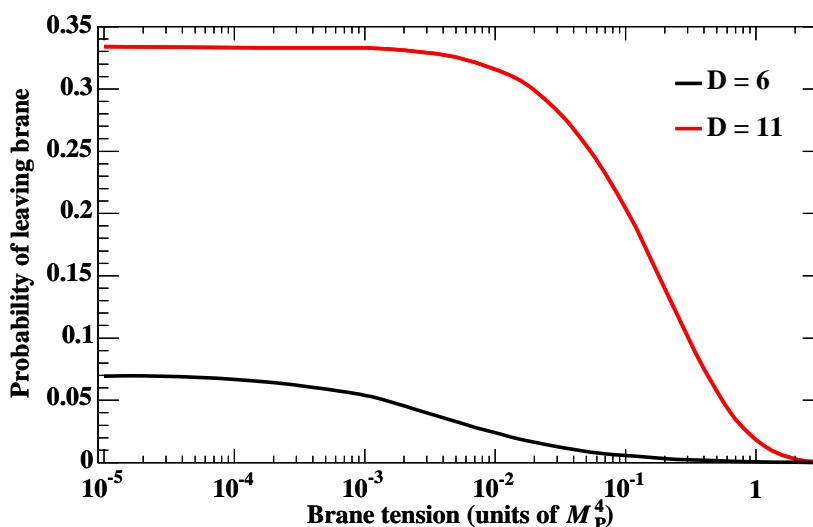


Figure 3: Probability per event that a black hole will leave the brane versus brane tension for $5 < M < 14$ TeV and $M_P = 1$ TeV. The black curve is for $D = 6$ while the red curve is for $D = 11$.

$M_P = 1$ TeV to leave the brane for different brane tensions $\hat{\sigma}$. The tension must be weak ($\hat{\sigma} < 1$) for the black hole to have a significant probability to leave the brane. In the extreme case of very weak tension ($\hat{\sigma} \rightarrow 0$), the probability becomes 6.9% for $D = 6$ and 33.4% for $D = 11$. In this case, the black hole will normally leave the brane as soon as the first graviton is emitted. We would expect similar shaped curves to figure 3 for different dimensions, Planck scales, and black hole masses. We might expect the probability to leave the brane at zero tension to increase in lower dimensions because of the increase in particle multiplicity. However, the probability of graviton emission per evaporated particle decreases with lower dimensions, so that the resulting probability per event for the black hole to leave the brane is lower in lower dimensions. Thus 33% is likely the maximum probability for black holes to leave the brane at LHC energies for $D \leq 11$.

6.3 Multiplicities

Multiplicities and emission probabilities for different particles, in particular the graviton, will be different for Hawking evaporation, the two-body final decay, and for events in which the black hole leaves the brane. Figure 4 show multiplicity distributions of primary particles emitted from black holes with $5 < M < 14$ TeV and $M_P = 1$ TeV for $D = 6$ (figure 4a) and $D = 11$ (figure 4b). These distributions include particles emitted by Hawking evaporation, as well as the two particles from the final decay. The black histograms are for all primary particles, and have means of 9.3 and 5.6 for $D = 6$ and $D = 11$. The red histograms in figure 4 are for the case of only visible primary particles when the black hole is allowed to leave the brane with $\hat{\sigma} = 0$. In this case, the mean multiplicities drop to 8.7 and 4.8 for $D = 6$ and $D = 11$, where the bin for zero multiplicity has not been included in the calculation of the means.

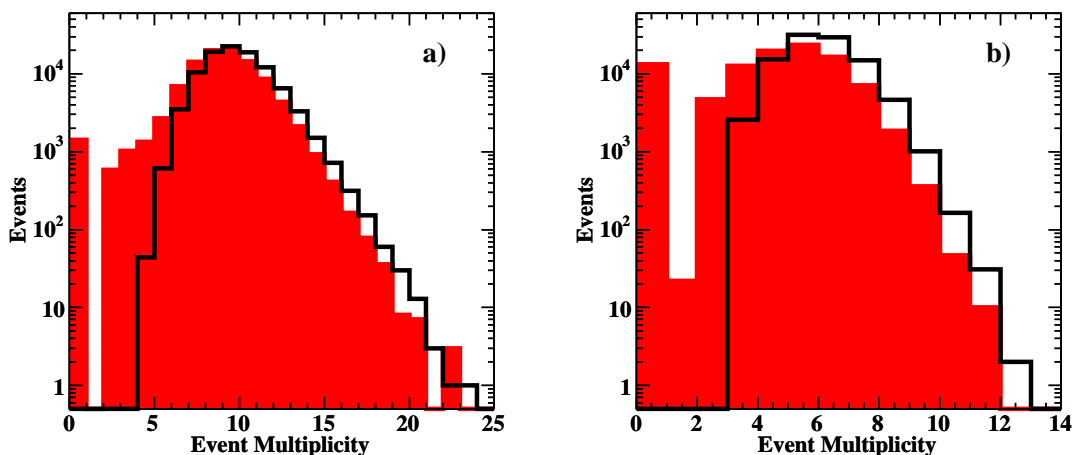


Figure 4: Multiplicity distributions of primary particles emitted from black holes with $5 < M < 14$ TeV and $M_P = 1$ TeV for a) $D = 6$ and b) $D = 11$. The black distributions are for all primary particles while the red distributions are for visible primary particles only and the black hole is allowed to leave the brane before the evaporation process is completed.

From the zero bins in figure 4, we see that 1.4% and 13.3% of the events will have no visible particles for $D = 6$ and $D = 11$. Most of these events correspond to the extreme case when the black hole emits a graviton as the first particle and immediately leaves the brane, with probabilities 1.4% and 12.8% for $D = 6$ and $D = 11$. It is also possible with probabilities 0.07% and 0.6% for $D = 6$ and $D = 11$ that the black hole first emits neutrinos and then a graviton, and leaves the brane. For these two cases, there would be no evidence that the black hole was ever formed or a proton-proton collision occurred. We would under-measure the black hole production rate and cross section by 1% and 13% for $D = 6$ and $D = 11$ with no possibility to correct the measurement based on the data itself.

Based on the average multiplicities and probability of graviton emission, we can estimate the asymptotic values in figure 3. For example, since the probability of emitting a graviton per emission is 12.8% and the mean multiplicity is 4.8 in 11 dimensions for $\hat{\sigma} = 0$, we estimate the probability per event to leave the brane is 35% which compares favourably with the simulated result of 33%.

Table 5 shows the percentage of gravitons produced in all events for strong tension $\hat{\sigma} = 10^3$ and zero tension. Multiple graviton emission per event in 11 dimensions is significant (4%) and comparable to single graviton emission in six dimensions (5%).

For comparison, we show the corresponding numbers for neutrinos in table 6. For $\hat{\sigma} = 10^3$, more particles are emitted so the multiplicity of neutrinos and multiple neutrino emission is higher than for the $\hat{\sigma} = 0$ case. For gravitons, the situation is reversed since the graviton ends the decay and thus inhibits other particles evaporating off the black hole.

We can understand the numbers in table 5 from the graviton emission probability and the particle multiplicities. Since the probability to leave the brane for $\hat{\sigma} = 0$ is equal to the probability for graviton emission, we can use the values in the $D = 11$ and $\hat{\sigma} = 0$

Number Gravitons	$D = 6$		$D = 8$		$D = 11$	
	$\hat{\sigma} = 10^3$	$\hat{\sigma} = 0$	$\hat{\sigma} = 10^3$	$\hat{\sigma} = 0$	$\hat{\sigma} = 10^3$	$\hat{\sigma} = 0$
0	94.8	92.2	89.3	85.9	69.1	61.3
1	5.0	7.8	10.2	14.1	26.4	38.6
2	0.1	0.0	0.5	0.0	4.2	0.2
3	0.0	0.0	0.0	0.0	0.4	0.0

Table 5: Percentage occurrence of various number of gravitons per event in black hole decay. For $\hat{\sigma} = 10^3$ the black hole does not leave the brane while for $\hat{\sigma} = 0$ the black hole may leave the brane.

Number Neutrinos	$D = 6$		$D = 8$		$D = 11$	
	$\hat{\sigma} = 10^3$	$\hat{\sigma} = 0$	$\hat{\sigma} = 10^3$	$\hat{\sigma} = 0$	$\hat{\sigma} = 10^3$	$\hat{\sigma} = 0$
0	61.5	62.9	73.7	75.8	80.0	84.3
1	30.1	29.2	22.9	21.0	18.2	14.3
2	7.2	6.8	3.1	2.9	1.7	1.3
3	1.0	1.0	0.3	0.2	0.1	0.1
4	0.1	0.1	0.0	0.0	0.0	0.0

Table 6: Percentage occurrence of various number of neutrinos per event in black hole decay. For $\hat{\sigma} = 10^3$ the black hole does not leave the brane while for $\hat{\sigma} = 0$ the black hole may leave the brane.

column of table 5 to estimate the probabilities of 0, 1, and 2 gravitons being emitted in the two-body final decay as 91.5%, 8.4%, and 0.3%. The values for strong brane tension in the $D = 11$ and $\hat{\sigma} = 10^3$ column can be understood as follows. Using the results for zero graviton emission, we predict a multiplicity of 3.2 for a graviton emission probability of 7.6% (table 3), or we predict a graviton emission probability of 7.5% assuming the mean multiplicity of 3.6. The multiplicity of 3.6 excludes the two particles from the final decay. The results are thus consistent with each other. Based on the 7.6% graviton emission probability and multiplicity of 3.6, we predict the probabilities of emitting 0, 1, 2, and 3 gravitons as 68.8%, 26.8%, 4.3%, and 0.4%. These predictions are consistent with the simulation results presented in table 5. We might expect multiple graviton emission to increase with multiplicity for lower dimensions, but the probability of a graviton per emission decreases with lower dimensions, and thus multiple graviton emission becomes even less in lower dimensions. Multiple graviton emission should occur at a level of less than 5% for any brane tension at the LHC provided $D \leq 11$.

6.4 Missing energy

Until now, we have been talking about missing energy which is due to undetectable particles on the brane or gravitons in the bulk. In proton-proton collisions, we neither know the initial-state energy or longitudinal momentum that went into producing the black hole. What we do know is that the transverse momentum to the proton beams is zero for the initial state. Thus the signature of missing energy can only be inferred by a non-zero total

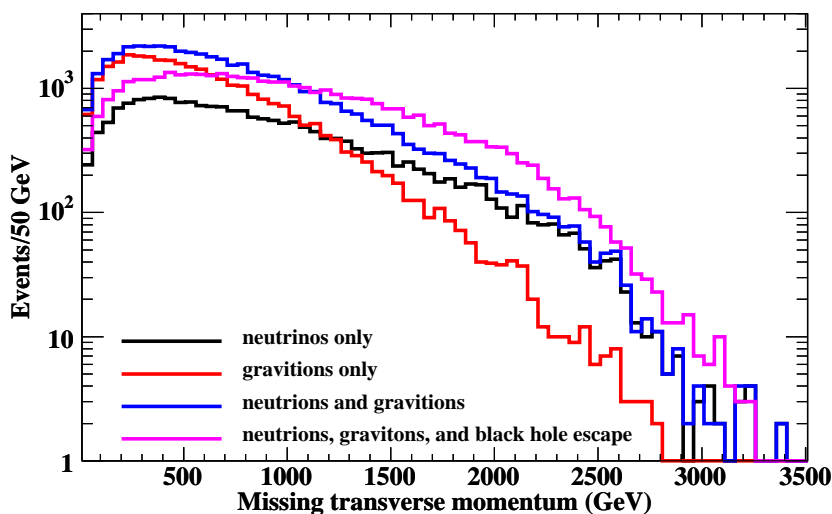


Figure 5: Missing transverse momentum for black holes with $5 < M < 14$ TeV, $M_P = 1$ TeV, and $D = 11$. The black histogram is due to neutrinos only, the red histogram is due to gravitons only, the blue histogram is due to neutrinos and gravitons while the magenta histogram is due to neutrinos, gravitons, and the possibility for the black hole to leave the brane. 100,000 events are in each histogram, but events with $\cancel{p}_T < 10$ GeV are zero suppressed.

transverse momentum in the event. In this section, we will be more precise and talk about missing transverse momentum \cancel{p}_T rather than missing energy.

Figure 5 shows the missing transverse momentum distribution for black holes with $5 < M < 14$ TeV, $M_P = 1$ TeV, and $D = 11$. The black histogram shows the case when \cancel{p}_T is due to the three generations of neutrinos only while the red histogram is the case for the gravitons only. The blue histogram is the case when the neutrinos and gravitons contribute to \cancel{p}_T , but the black hole is not allowed to leave the brane ($\hat{\sigma} = 10^3$). The magenta histogram is the case when the black hole is allowed to leave the brane with a vanishing brane tension. Events which do not emit neutrinos or gravitons (55%) are not included in the histogram. Some events emit a graviton as the first particle, and the black hole leaves the brane without emitting a Standard Model particle. These events have $\cancel{p}_T = 0$ and are also not included in the histogram. More events have missing transverse momentum due to neutrinos than gravitons, and the value of \cancel{p}_T from neutrinos is higher because all of the momentum components for the neutrino are on the brane. Allowing the black hole to escape from the brane increases the mean missing transverse momentum considerably to 960 GeV for 38% of the events. The other 62% of the events have no significant \cancel{p}_T . The missing transverse momentum decreases to 530 GeV in six dimensions for 42% of the events. In this case, the missing transverse momentum is predominated due to neutrinos.

The missing transverse momentum distributions in figure 5 are consistent with previous results that include the neutrinos only and detector effects [16]. The black hole missing transverse momentum distributions for 11 dimensions are very different from QCD and

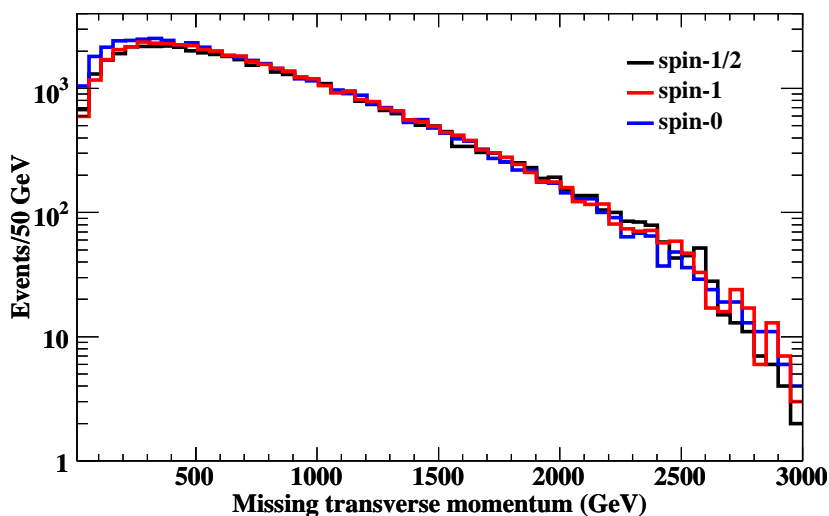


Figure 6: Missing transverse momentum for black holes with $5 < M < 14$ TeV, $M_P = 1$ TeV, and $D = 11$ for different graviton grey-body spectra. The black histogram is for a spin-1/2 spectrum, the red histogram is for a spin-1 spectrum while the blue histogram is for a spin-0 spectrum. 100,000 events are in each histogram, but events with $p_T < 10$ GeV are zero suppressed.

SUSY events [16].

The missing transverse momentum distribution is not very sensitive to our choice of graviton energy spectrum. Figure 6 shows the missing transverse momentum distribution due to neutrinos and gravitons only for different grey-body spectra for the graviton. The black histogram is for a spin-1/2 spectrum, the red histogram is for a spin-1 spectrum while the blue histogram is for a spin-0 spectrum. Thus, we are insensitive to the choice of graviton spectrum provided $p_T \gtrsim 300$ GeV.

6.5 Mass and cross section

We can ask how graviton emission and black hole recoil affect experimental measurements? An experiment needs to first identify black hole events and then measure the black hole mass. We will assume the black hole events are well identified by their decay to high- p_T objects and possibly missing energy. However, events with no or little visible energy will not be identified as black hole events, or events of any type. Based on the multiplicity distribution, we expect a maximum of 13% of the black hole events to fall into this category for $D \leq 11$.

Having identified the black hole events, we now need to reconstruct their masses. Since the black hole mass is reconstructed by summing the four-vectors of all the particles, missing energy will result in decreasing the reconstructed black hole masses. However, events without neutrinos or gravitons should have well reconstructed mass. We expect about 60% of the events in 11 dimensions will not be affected by missing energy. Figure 7 shows the reconstructed black hole mass versus missing transverse momentum in 11 dimensions for vanishing brane tension.

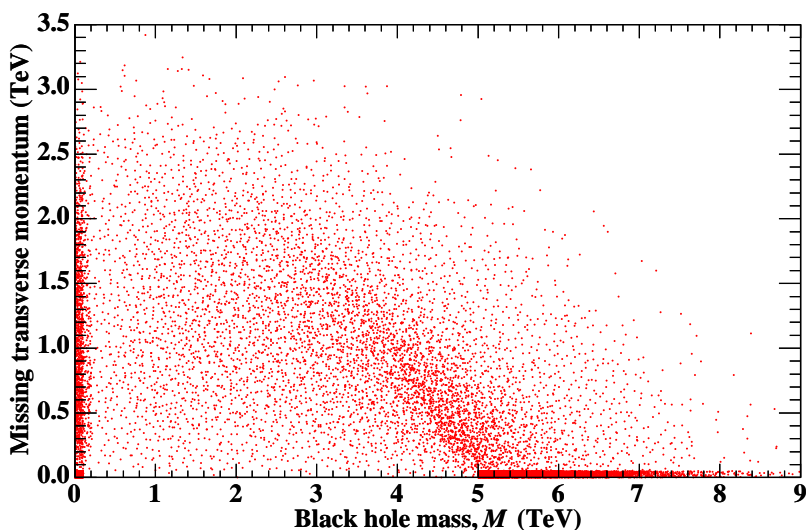


Figure 7: Black hole mass versus missing transverse momentum for black holes with $5 < M < 14$ TeV, $M_P = 1$ TeV, $D = 11$, and vanishing brane tension.

In events with missing energy, the reconstructed mass will always be low. Black holes with mass near 5 TeV will be reconstructed with masses that fall outside the $5 < M < 14$ TeV mass window we are considering. Black holes with mass well above 5 TeV will also be reconstructed with lower masses but remain within the mass window we are considering. Because of the steeply falling cross section with black hole mass, the problem of migration of high-mass values to lower masses within our mass window will be less significant than the number of events migrating out of the mass window below 5 TeV. The net effect will be to decrease the total number of events reconstructed and the shape of the differential cross section. Selecting only events with low missing energy will decrease its effect on the mass reconstruction and cross section determination.

As an illustrative example, we have required $\cancel{p}_T < 10$ GeV and plotted the differential cross section versus black hole mass with and without missing energy as shown in figure 8. The exact value for the missing energy cut will have to be determined from a full simulation of the detector and the data. The shape of the cross section changes only slightly at high masses, where there are few events. The contamination of any mass bin due the migration of higher-mass events was determined from the simulation to be of the order of 0.01%.

The cross section for black hole production with $5 < M < 14$ TeV, $M_P = 1$ TeV, and $D = 11$ is 24 pb, for the default parton density functions used by PYTHIA. Integrating the differential cross section for missing energy events (red histogram) in figure 8 gives a reduced cross section of 13 pb (12 pb before acceptance correction). Although this is only a reduction in the theoretical cross section of about 50%, such an error could make the determination of the Planck scale and number of dimensions difficult. It may be possible to improve the mass resolution by treating the missing transverse momentum as a massless pseudo-particle in the calculation of the black hole mass. To go further in these studies,

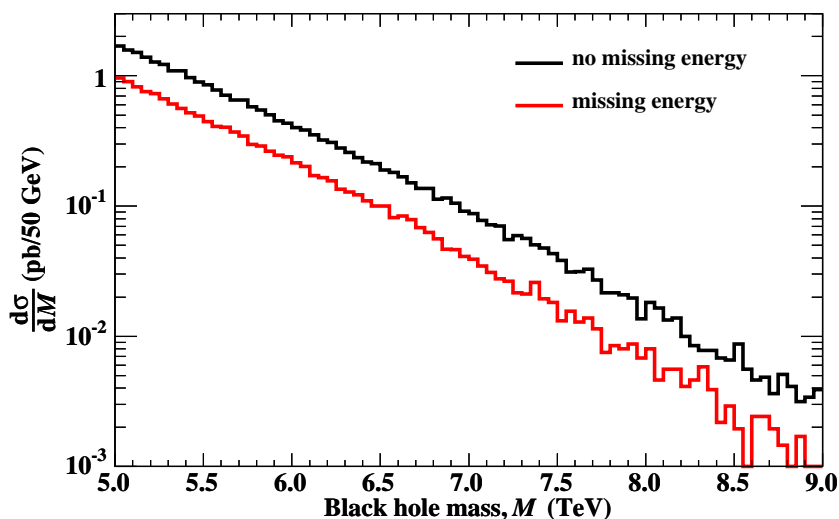


Figure 8: Differential cross section for black holes with $5 < M < 14$ TeV, $M_P = 1$ TeV, and $D = 11$. The black histogram is the perfect situation in which we can unrealistically determine the exact black hole mass. The red histogram is due to undetected neutrinos, gravitons, and the possibility for the black hole to leave the brane.

will require including particle fragmentation, hadronization, decay, and detector effects. For example, the limit geometrical acceptance of detectors and heavy-particle decays will further contribute to the missing energy.

7. Discussion

We now discuss some of our assumptions. We have assumed the validity of a next to probe-brane approximation. For this assumption to be valid, the mass of the portion of the brane near the black hole horizon must be much smaller than the black hole mass $\sigma r_h^3 \ll M$ [49]. This conditions translates to

$$\hat{\sigma} \ll \left(\frac{M}{M_P} \right)^{\frac{D-6}{D-3}}. \tag{7.1}$$

So the next to probe-brane approximation will be valid until $M \sim M_P$, ie. if $\hat{\sigma} \ll 1$.

Energy-momentum conservation in four dimensions is a result of translational invariance in four-dimensional spacetime. The three-brane breaks the translational invariance in the extra dimensions and hence momentum in these directions need not be conserved in interactions between the bulk and brane states. Nevertheless, we have assumed energy-momentum conservation between the gravitons and the black hole in all the dimensions.

We have generated black holes with mass well above the Planck scale in order to work in the regime of classical gravity. However, the black hole eventually decays down to the Planck scale and quantum gravity probably becomes important. The effects of black hole recoil are most significant near the Planck scale. Thus black holes may behave differently

than we have depicted, but we might expect the concepts of black hole recoil and missing energy to remain unchanged.

The studies presented here do not include parton fragmentation, hadronization, decay, detector effects, or backgrounds. Including these effects is likely to change the missing energy and mass distributions for black hole events. However, it is anticipated that the qualitative results for the missing energy, black hole mass, and cross section will remain unchanged.

We draw two conclusions from our study of missing energy in black hole evaporation:

1. black holes will leave the brane less than 1/3 of the time at the LHC, and
2. for very weak brane tensions, the irreducible acceptance for the detection of black holes above 5 TeV can be as low as 87%.

We have only studied the missing energy in black hole evaporation. Missing energy from graviton emission during and shortly after black hole formation could be more significant. This graviton emission will have to be better understood before the cross section can be measured and the Planck scale and number of dimensions determined.

Acknowledgments

This work was supported in part by the Natural Sciences and Engineering Research Council of Canada, and the Faculty of Science University College London. I thank the Flower Kings for inspiration.

References

- [1] N. Arkani-Hamed, S. Dimopoulos and G.R. Dvali, *The hierarchy problem and new dimensions at a millimeter*, *Phys. Lett.* **B 429** (1998) 263 [[hep-ph/9803315](#)].
- [2] I. Antoniadis, N. Arkani-Hamed, S. Dimopoulos and G.R. Dvali, *New dimensions at a millimeter to a Fermi and superstrings at a TeV*, *Phys. Lett.* **B 436** (1998) 257 [[hep-ph/9804398](#)].
- [3] N. Arkani-Hamed, S. Dimopoulos and G.R. Dvali, *Phenomenology, astrophysics and cosmology of theories with sub-millimeter dimensions and TeV scale quantum gravity*, *Phys. Rev.* **D 59** (1999) 086004 [[hep-ph/9807344](#)].
- [4] S.W. Hawking, *Particle creation by black holes*, *Commun. Math. Phys.* **43** (1975) 199.
- [5] S. Dimopoulos and R. Emparan, *String balls at the LHC and beyond*, *Phys. Lett.* **B 526** (2002) 393 [[hep-ph/0108060](#)].
- [6] K. Cheung, *Black hole, string ball and p-brane production at hadronic supercolliders*, *Phys. Rev.* **D 66** (2002) 036007 [[hep-ph/0205033](#)].
- [7] H. Yoshino and R.B. Mann, *Black hole formation in the head-on collision of ultrarelativistic charges*, *Phys. Rev.* **D 74** (2006) 044003 [[gr-qc/0605131](#)].
- [8] D.M. Gingrich, *Effect of charged partons on black hole production at the Large Hadron Collider*, *JHEP* **02** (2007) 098 [[hep-ph/0612105](#)].

- [9] H. Yoshino and V.S. Rychkov, *Improved analysis of black hole formation in high-energy particle collisions*, *Phys. Rev. D* **71** (2005) 104028 [[hep-th/0503171](#)].
- [10] D.M. Gingrich, *Black hole cross section at the Large Hadron Collider*, *Int. J. Mod. Phys. A* **21** (2006) 6653 [[hep-ph/0609055](#)].
- [11] P.D. D'Eath, *Gravitational radiation in high-speed black-hole collisions*, *Class. and Quant. Grav.* **10** (1993) S207.
- [12] T. Banks and W. Fischler, *A model for high energy scattering in quantum gravity*, [hep-th/9906038](#).
- [13] S. Dimopoulos and G.L. Landsberg, *Black holes at the LHC*, *Phys. Rev. Lett.* **87** (2001) 161602 [[hep-ph/0106295](#)].
- [14] S.B. Giddings and S.D. Thomas, *High energy colliders as black hole factories: the end of short distance physics*, *Phys. Rev. D* **65** (2002) 056010 [[hep-ph/0106219](#)].
- [15] G.L. Landsberg, *Discovering new physics in the decays of black holes*, *Phys. Rev. Lett.* **88** (2002) 181801 [[hep-ph/0112061](#)].
- [16] C.M. Harris et al., *Exploring higher dimensional black holes at the Large Hadron Collider*, *JHEP* **05** (2005) 053 [[hep-ph/0411022](#)].
- [17] J. Tanaka, T. Yamamura, S. Asai and J. Kanzaki, *Study of black holes with the ATLAS detector at the LHC*, *Eur. Phys. J. C* **41** (2005) 19 [[hep-ph/0411095](#)].
- [18] B. Koch, M. Bleicher and S. Hossenfelder, *Black hole remnants at the LHC*, *JHEP* **10** (2005) 053 [[hep-ph/0507138](#)].
- [19] A. Casher and N. Raz, *On black hole remnants*, [arXiv:0705.0444](#).
- [20] S.W. Hawking, *Information loss in black holes*, *Phys. Rev. D* **72** (2005) 084013 [[hep-th/0507171](#)].
- [21] D.N. Page, *Particle emission rates from a black hole. 2. Massless particles from a rotating hole*, *Phys. Rev. D* **14** (1976) 3260.
- [22] M. Casals, S.R. Dolan, P. Kanti and E. Winstanley, *Brane decay of a $(4+n)$ -dimensional rotating black hole. III: spin-1/2 particles*, *JHEP* **03** (2007) 019 [[hep-th/0608193](#)].
- [23] D. Ida, K.-Y. Oda and S.C. Park, *Rotating black holes at future colliders. III: determination of black hole evolution*, *Phys. Rev. D* **73** (2006) 124022 [[hep-th/0602188](#)].
- [24] D.N. Page, *Particle emission rates from a black hole: massless particles from an uncharged, nonrotating hole*, *Phys. Rev. D* **13** (1976) 198.
- [25] F. Pretorius and D. Khurana, *Black hole mergers and unstable circular orbits*, *Class. and Quant. Grav.* **24** (2007) S83 [[gr-qc/0702084](#)].
- [26] H. Elvang, R. Emparan and P. Figueras, *Phases of five-dimensional black holes*, *JHEP* **05** (2007) 056 [[hep-th/0702111](#)].
- [27] D. Ida, K.-Y. Oda and S.C. Park, *Rotating black holes/rings at future colliders*, [hep-ph/0312061](#).
- [28] R. Emparan, G.T. Horowitz and R.C. Myers, *Black holes radiate mainly on the brane*, *Phys. Rev. Lett.* **85** (2000) 499 [[hep-th/0003118](#)].

- [29] M. Cavaglia, *Black hole multiplicity at particle colliders (do black holes radiate mainly on the brane?)*, *Phys. Lett.* **B 569** (2003) 7 [[hep-ph/0305256](#)].
- [30] D.K. Park, *Emissivities for the various graviton modes in the background of the higher-dimensional black hole*, *Phys. Lett.* **B 638** (2006) 246 [[hep-th/0603224](#)].
- [31] S. Creek, O. Eftimiou, P. Kanti and K. Tamvakis, *Graviton emission in the bulk from a higher-dimensional Schwarzschild black hole*, *Phys. Lett.* **B 635** (2006) 39 [[hep-th/0601126](#)].
- [32] P. Kanti and J. March-Russell, *Calculable corrections to brane black hole decay. I: the scalar case*, *Phys. Rev.* **D 66** (2002) 024023 [[hep-ph/0203223](#)].
- [33] P. Kanti and J. March-Russell, *Calculable corrections to brane black hole decay. II: greybody factors for spin 1/2 and 1*, *Phys. Rev.* **D 67** (2003) 104019 [[hep-ph/0212199](#)].
- [34] C.M. Harris and P. Kanti, *Hawking radiation from a $(4+n)$ -dimensional black hole: exact results for the Schwarzschild phase*, *JHEP* **10** (2003) 014 [[hep-ph/0309054](#)].
- [35] P. Kanti, *Black holes in theories with large extra dimensions: a review*, *Int. J. Mod. Phys.* **A 19** (2004) 4899 [[hep-ph/0402168](#)].
- [36] D. Ida, K.-Y. Oda and S.C. Park, *Rotating black holes at future colliders. II: anisotropic scalar field emission*, *Phys. Rev.* **D 71** (2005) 124039 [[hep-th/0503052](#)].
- [37] D. Ida, K.-Y. Oda and S.C. Park, *Rotating black holes at future colliders: greybody factors for brane fields*, *Phys. Rev.* **D 67** (2003) 064025 [[hep-th/0212108](#)].
- [38] G. Duffy, C. Harris, P. Kanti and E. Winstanley, *Brane decay of a $(4+n)$ -dimensional rotating black hole: spin-0 particles*, *JHEP* **09** (2005) 049 [[hep-th/0507274](#)].
- [39] M. Casals, P. Kanti and E. Winstanley, *Brane decay of a $(4+n)$ -dimensional rotating black hole. II: spin-1 particles*, *JHEP* **02** (2006) 051 [[hep-th/0511163](#)].
- [40] D.K. Park, *Hawking radiation of the brane-localized graviton from a $(4+n)$ -dimensional black hole*, *Class. and Quant. Grav.* **23** (2006) 4101 [[hep-th/0512021](#)].
- [41] V. Cardoso, M. Cavaglià and L. Gualtieri, *Black hole particle emission in higher-dimensional spacetime*, *Phys. Rev. Lett.* **96** (2006) 071301 [*Erratum ibid.* **96** (2006) 219902] [[hep-ph/0512002](#)].
- [42] V. Cardoso, M. Cavaglia and L. Gualtieri, *Hawking emission of gravitons in higher dimensions: non-rotating black holes*, *JHEP* **02** (2006) 021 [[hep-th/0512116](#)].
- [43] G.L. Landsberg, *Black holes at future colliders and beyond: a review*, [hep-ph/0211043](#).
- [44] V.P. Frolov, M. Snajdr and D. Stojković, *Interaction of a brane with a moving bulk black hole*, *Phys. Rev.* **D 68** (2003) 044002 [[gr-qc/0304083](#)].
- [45] V.P. Frolov and D. Stojković, *Black hole as a point radiator and recoil effect on the brane world*, *Phys. Rev. Lett.* **89** (2002) 151302 [[hep-th/0208102](#)].
- [46] V.P. Frolov and D. Stojković, *Black hole radiation in the brane world and recoil effect*, *Phys. Rev.* **D 66** (2002) 084002 [[hep-th/0206046](#)].
- [47] A. Flachi, O. Pujolàs, M. Sasaki and T. Tanaka, *Dynamics of domain walls intersecting black holes*, [hep-th/0601174](#).
- [48] A. Flachi and T. Tanaka, *Escape of black holes from the brane*, *Phys. Rev. Lett.* **95** (2005) 161302 [[hep-th/0506145](#)].

- [49] A. Flachi, O. Pujolàs, M. Sasaki and T. Tanaka, *Critical escape velocity of black holes from branes*, *Phys. Rev. D* **74** (2006) 045013 [[hep-th/0604139](#)].
- [50] G.R. Dvali, G. Gabadadze, M. Kolanovic and F. Nitti, *Scales of gravity*, *Phys. Rev. D* **65** (2002) 024031 [[hep-th/0106058](#)].
- [51] H. Murayama and J.D. Wells, *Graviton emission from a soft brane*, *Phys. Rev. D* **65** (2002) 056011 [[hep-ph/0109004](#)].
- [52] C.M. Harris, P. Richardson and B.R. Webber, *CHARYBDIS: a black hole event generator*, *JHEP* **08** (2003) 033 [[hep-ph/0307305](#)].
- [53] D.M. Gingrich, *Comparison of black hole generators for the LHC*, [hep-ph/0610219](#).